

OPTIMIZATION OF HEAT TREATMENT OF Nd-Fe-B-BASED ALLOYS FOR PREPARATION OF HIGH COERCIVITY PERMANENT MAGNETS

KOSHKID'KO Yurij S.^{1,2}, SKOTNICOVÁ Kateřina¹, ČEGAN Tomáš¹, LESŇÁK Michal¹, ŽIVOTSKÝ Ondřej¹, HRABOVSKÁ Kamila¹, MAMULOVÁ KUTLÁKOVÁ Kateřina³, LUKIN Alexander A.⁴, DORMIDONTOV Andrey G.⁴, SITNOV VLADIMIR V.⁴, KOLCHUGINA Natalia B.⁵, CWIK Jacek², SNÁŠELOVÁ Lucie¹

¹VSB - Technical University of Ostrava, Faculty of Metallurgy and Materials Engineering, Regional Materials Science and Technology Centre, Ostrava, Czech Republic, EU, Katerina.Skotnicova@vsb.cz

²International Laboratory of High Magnetic Fields and Low Temperatures, Wrocław, Poland, EU, cwikjac@ml.pan.wroc.pl

³VSB - Technical University of Ostrava, Nanotechnology Centre, Ostrava, Czech Republic, EU

⁴JSC SPETSMAGNIT, Moscow, Russian Federation, lukinikul@rambler.ru

⁵Baikov Institute of Metallurgy and Materials Science, Russian Academy of Sciences, Moscow, Russian Federation, natalik@imet.ac.ru

Abstract

Optimization of conditions of heat treatment of Nd-Fe-B-based permanent magnets, prepared using the strip casting method, was carried out with the aim to enhance their coercivity H_{CJ} and maximal energy product $(BH)_{max}$, and to improve the shape of the demagnetization curve. The initial alloy with the chemical composition (for high-coercivity magnets) of Fe - 67.05; Nd - 19.50; B - 1; Dy - 6.00; Pr - 6.00; Cu - 0.15; Al - 0.30 (wt.%) in form of strips was submitted to hydrogen decrepitation and vibration milling. The obtained powder with the granulometry of 3-5 μm was mixed with 2.5 wt.% NdH_2 in order to improve the liquid phase sintering process and to increase the coercivity as a result of formation of continuous grain boundary. Structural characteristics and phase composition were investigated using scanning electron microscopy equipped with EDX microprobe, light optical microscopy equipped with digital camera and XRPD. The microhardness of the principal $\text{Nd}(\text{R})_2\text{Fe}_{14}\text{B}$ phase was measured. Magnetic properties were evaluated using automatic hysteresisgraph and vibrating-sample magnetometer. The maximal values of the coercive force H_{CJ} of $1470 \text{ kA}\cdot\text{m}^{-1}$ were achieved by the heat treatment at $500 \text{ }^\circ\text{C}$. An increase of this temperature to $550 \text{ }^\circ\text{C}$ led to a sharp drop in magnetic properties and microhardness. The magneto-optical Kerr microscopy was used to visualize the magnetic domain patterns on the surface of magnetic materials. The observed star-like domain structure indicates a good magnetic texture for permanent magnets. These data are of great importance for choosing the optimum heat treatment of Nd-Fe-B-based magnets.

Keywords: Nd-Fe-B permanent magnets, strip casting, magnetic domain structure, X-ray diffraction analysis

1. INTRODUCTION

Sintered Nd-Fe-B magnets find wide applications in technology thanks to the high maximum energy product $(BH)_{max}$, residual inductance (B_r), and magnetization coercive force (H_{CJ}). Nd-Fe-B permanent magnets are used in many fields of industry. One of the problems of use of permanent magnets based on the $\text{Nd}_2\text{Fe}_{14}\text{B}$ compound is the preservation of high magnetic properties at high temperatures. Addition of heavy rare earths of Dy or Tb effectively enhances coercivity and consequent thermal stability of the Nd-Fe-B magnets, because Dy or Tb increases the magnetic anisotropy field of the $\text{Nd}_2\text{Fe}_{14}\text{B}$ compound [1-2]. However, the search of the optimal composition for the magnetic properties and the preparation of technological process for manufacture of permanent magnets is difficult. Some of these problems can be solved using the technology of strip casting.

However, during the milling process a partial oxidation of the phase rich in rare earth metals can occur. This may lead to a deterioration of liquid phase sintering process due to the reduced amount of liquid phase. Formation of grain boundaries thus becomes difficult. This can lead to a decrease of the coercive force of permanent magnets, because a H_{cJ} value largely depends on the state of the grain boundaries [3-5]. This problem can be partly solved by selecting the optimum heat treatment. However, this is not enough. For this reason, the authors of this article proposed to add a hydride rare earth metal at the milling step. In addition, the authors have determined the optimal heat treatment for the developed highly coercive magnet.

2. EXPERIMENTAL

The initial alloy with the chemical composition of Fe - 67.05; Nd - 19.50; B - 1; Dy - 6.00; Pr - 6.00; Cu - 0.15; Al - 0.30 (wt.%) was prepared by vacuum induction melting followed by the pouring of melt on water-cooled rotating copper wheel ($v = 1.5\text{-}2 \text{ m}\cdot\text{s}^{-1}$). This "Strip Casting" method is used to prevent the formation of long dendrites of magnetically soft phase α -Fe, and to achieve more homogeneity and finer scale microstructures which require less rare-earth metals. The material obtained in the form of strips with thickness from 300 to 500 μm was then subjected to hydrogen decrepitation for 1-2 h at a "dry" hydrogen pressure of 0.1 MPa; the subsequent cooling was realized at room temperature in a nitrogen atmosphere. The milling using a vibration mill was carried out in isopropyl alcohol. Neodymium hydride (2.5 wt.%) was added at the grinding stage in order to improve sintering of the liquid-phase. The mean powder particle size was 3-5 μm . The pressing force was 1.5-2 t/cm² at a magnetic field of 2 T (pressing of parts in transverse field). The sintering was carried out at 1080 °C for 2 h (Sample N0). In search of the optimum conditions of heat-treatment, annealing was performed progressively at 500 °C (Sample N1), 530 °C (Sample N2), 550 °C (Sample N3) for 1 h each. After each stage, the gas (nitrogen, argon) quenching was carried out. Magnetic properties of the samples of permanent magnet were measured using a hysteresisgraph HG 200 and vibrating sample magnetometer, which was carried out in the International Laboratory of High Magnetic Fields and Low Temperatures in Wroclaw (Poland). The high-resolution field emission gun-scanning electron microscope QUANTA 450 FEG equipped with an EDX APOLLO X microprobe was applied for the investigation of microstructure and chemical composition of samples [6]. The XRPD patterns were recorded under $\text{CoK}\alpha$ irradiation ($\lambda = 0.1789 \text{ nm}$) using the Bruker D8 Advance diffractometer (Bruker AXS) equipped with a fast position sensitive detector VANTEC 1. Measurements were carried out in the reflection mode, powder samples were pressed in a rotational holder. The magneto-optical Kerr microscopy was used to visualize the magnetic domain patterns on the surface of magnetic materials.

3. RESULTS AND DISCUSSION

3.1. SEM/EDX analysis

The stoichiometric composition of grains in all samples is close to that of the $\text{Nd}_2\text{Fe}_{14}\text{B}$ phase (Phase 1 in **Fig. 1**). The ideal Fe/R ratio ($R = \text{Dy, Pr, Dy}$) should be ~ 7 . However, as is seen from the calculation of the Fe/R ratio in **Table 1**, some differences take place. This is related to the existence of errors of determination of the phase composition, which are due to the closeness of characteristic X-ray spectra of some elements. In particular, the excitation potential for the L_α - series of Dy is 6.494 keV, whereas for Fe, the excitation potential for Fe K_α is 6.403 keV. Therefore, we must take spectra with the lower intensity; this can give error in determining the quantitative phase composition of material. In case of Dy, we used the $M\alpha$ (1.293 keV) characteristic radiation. Another difficulty exists in determining the chemical composition for the area (since the electron beam diameter is $\sim 2 \mu\text{m}$).

Based on the analysis of chemical composition, the presence of REM oxide phases in ternary junctions of samples is assumed (Phase 2 and 3 in **Fig. 1**). According to literature data [7-9], ternary junctions can contain different oxide phases. These are NdO (the oxygen content is 50 at.%), Nd_2O_3 (the oxygen content is 60 at.%)

[9-10], and NdO₂ (the oxygen content is 67 at.%) [3].

The atomic percentage of elements in ternary junctions corresponds to phases with the stoichiometric compositions close to the Nd₂O₃ or NdO phases. The presence of these phases in the samples was also confirmed by the X-ray diffraction analysis data.

Table 1 Average chemical composition of phases observed in samples N0-N3 (at.%)

Sample	Phase	OK	DyM	AlK	TiK	PrL	NdL	FeK	CoK	CuK	Fe/R ratio
N0	1	7.26	2.14	1.55	0.29	2.78	9.29	75.91	0.27	0.51	5.52
	2	45.68	3.04	0.59	0.31	7.14	19.89	23.09	0.11	0.17	
	3	56.69	2.25	0.20	0.13	7.30	21.57	11.65	0.00	0.21	
N1	1	8.12	2.12	1.32	0.27	2.17	9.55	75.41	0.52	0.51	5.64
	2	44.54	3.115	0.735	0.26	6.115	18.96	25.96	0	0.32	
	3	48.04	2.69	0.98	0.25	6.13	18.81	22.72	0	0.38	
N2	1	7.79	2.62	1.68	0.33	2.46	8.62	75.79	0.17	0.54	5.73
	2	48.86	2.69	0.07	0.23	7.18	21.00	19.52	0.00	0.45	
	3	63.44	2.30	0.15	0.21	4.55	13.52	14.60	0.58	0.65	
N3	1	8.69	2.52	1.26	0.24	2.46	8.4	75.41	0.37	0.66	5.82
	2	46.35	3.64	0.18	0.36	7.30	22.55	18.60	0.31	0.72	
	3	33.59	2.44	0.62	0.22	3.40	11.02	48.17	0.12	0.43	

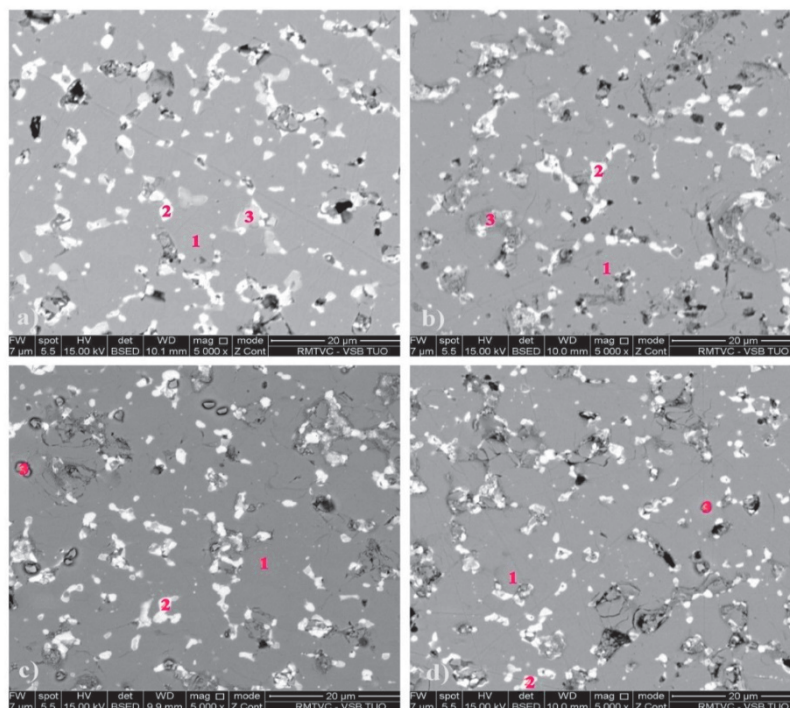


Fig. 1 SEM image of N0 (a), N1 (b), N2 (c) and N3 (d) samples with marking of analyzed phases

3.2. X-ray diffraction analysis

Fig. 2 demonstrates the comparison of experimental X-ray diffraction pattern (colored lines) and pattern simulated for the Nd₂Fe₁₄B-type structure (space group P42/mnm) (black lines). It can be seen that main

reflections simulated for the Nd₂Fe₁₄B coincide adequately with those in the experimental X-ray diffraction pattern; some reflections are likely to belong to other phases. These reflections are observed at 2 Θ angles of 35.59; 36.07 and 49.97 deg. Subsequent analysis of experimental X-ray diffraction patterns was performed in detail using literature data and simulated X-ray diffraction patterns. It is known from literature that the presence of α -Fe phase can affect the properties of permanent magnets [5]. However, we failed to detect the α -Fe phase at the background of reflections of the Nd₂Fe₁₄B phase. The presence of the α -Fe phase in all four samples could be revealed by thermal magnetic analysis. Based on the analysis of chemical composition and literature data [7-9], we assumed the presence of REM oxide phases in ternary junctions of investigated samples. According to the literature data, ternary junctions can contain different oxide phases. These are NdO with the NaCl-type structure (space group Fm-3m) [9] (the oxygen content is 50 at.%), Nd₂O₃ with the La₂O₃-type structure (space group Pm-3m) (the oxygen content is 60 at.%) [2, 3], and NdO₂ with the CaF₂-type structure (space group Fm-3m) (the oxygen content is 67 at.%) [9].

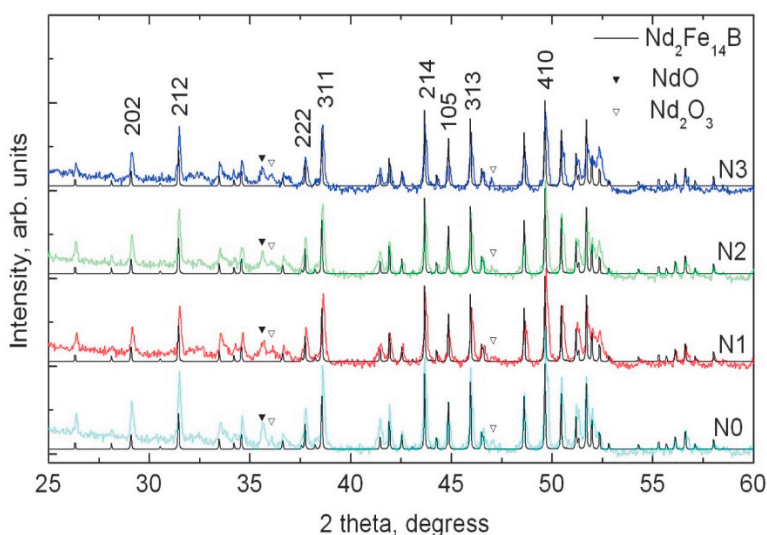


Fig. 2 X-ray diffraction pattern for the sample N0, N1, N2 and N3 ($\lambda = 0.1789$ nm)

The patterns in **Fig. 2**, simulated for the structures of the NdO and Nd₂O₃ oxides, agree adequately with the experimental patterns. A slight difference can be explained by the fact that the simulation was performed for the NdO and Nd₂O₃ compounds, whereas, according to chemical analysis data, these compounds can contain Dy and Pr, i.e., and they can differ from the composition preset by the simulation program.

Moreover, we found the shift of reflections for the samples N0-3 relatively to each other (**Fig. 2**). This is possibly related to the changes in the lattice parameters of the principal Nd₂Fe₁₄B phase. The calculated lattice parameters of the phase are given in **Table 2**.

Table 2 Calculated lattice parameters for the phase with the Nd₂Fe₁₄B-type structure for all samples

Sample	a (nm)	c (nm)	c/a
N0	0.87940	1.21923	1.386
N1	0.87933	1.21934	1.386
N2	0.87929	1.21975	1.387
N3	0.87941	1.22007	1.387

For the sample N3 the peak of the oxide phase significantly increased. This might have been caused by the increased number of the oxide phase. Modification of the lattice parameter is associated with diffusion of atoms from the phase rich in rare earth metals in the grain.

3.3. Magnetic properties

Preliminary studies of magnetic properties with use of magnetic hysteresis graph showed that the sample N1 has the best magnetic properties. However the value of the coercive force exceeds the limits of measuring of the magnetic field for hysteresis graph (1465 kA·m⁻¹). Therefore, a more detailed study of the magnetic properties of the sample N1 was conducted using a vibrating sample magnetometer.

Fig. 3a shows the demagnetization curve for the sample of the permanent magnet N1. This curve was constructed from the experimental data obtained by using a vibrating sample magnetometer. When constructing the demagnetization curve, the demagnetizing field of the sample was taken into account. **Fig. 3b** demonstrates the determination of the maximum energy product $(BH)_{max}$. As it can be seen from the graph, this value reaches $(BH)_{max} = 231 \text{ kJ}\cdot\text{m}^{-3}$, which is typical for high-coercivity magnets. The basic magnetic properties of the sample of the permanent magnet N1 are shown in **Table 3**.

Further increase in the temperature of heat treatment reduces the value of the coercive force. For the sample N3, it can be seen that as a result of heat treatment at 550 °C a sharp drop in coercive force occurred. Perhaps this is due to the process of formation of grain boundaries during heat treatment or to an increase of the oxide phase. It also confirms the decrease in the microhardness of the sample N3 (**Table 4**).

Table 3 Magnetic properties of the permanent magnet N1 (heat treatment at 500 °C).

B_r	H_{cJ}	H_{cB}	H_k	$(BH)_{max}$
T	kA·m ⁻¹	kA·m ⁻¹	kA·m ⁻¹	kJ·m ⁻³
1.1	1470	808	909	231

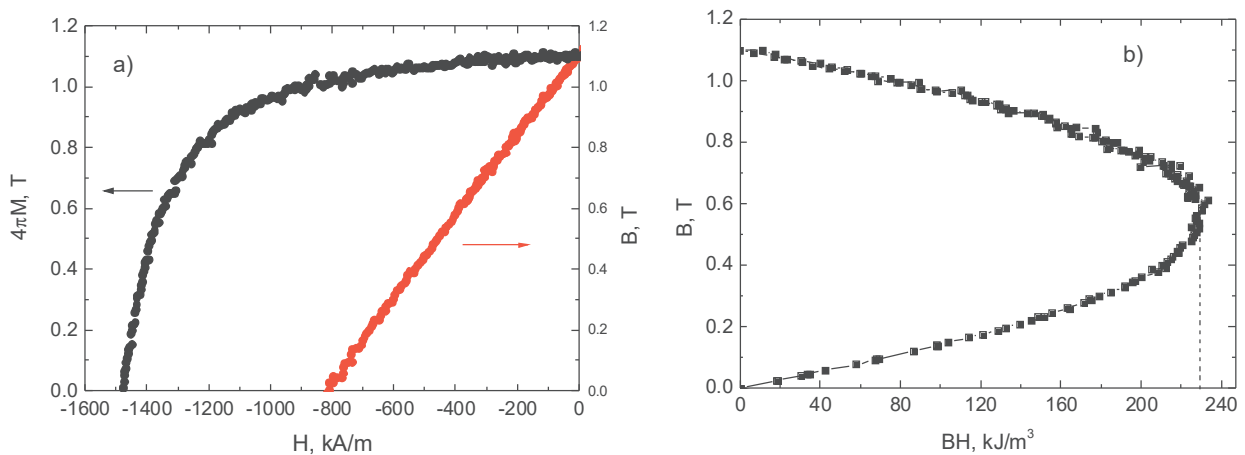


Fig. 3 Magnetic properties of the sample of the permanent magnet N1 at room temperature: a) demagnetization curves, b) the dependence of B on BH

Table 4 Microhardness of the N0, N1, N2 and N3 samples

Samle	$HV_{av} (-)$
N ₀	611.7 ± 101.5
N ₁	524.3 ± 97.2
N ₂	535.3 ± 98.5
N ₃	397.7 ± 41.7

3.4. Structure of magnetic domains

The domain structure of the samples of permanent magnets was observed at low magnetic fields (practically in remnant state). Investigations were conducted at the Institute of Physics (VSB-TUO). Study of the structure of magnetic domain was carried out on the sample surface, which was perpendicular to the axis of the texture. Red squares in **Fig. 4** highlight the areas, where the magnetic domain structure of sample N1 was observed. The domain structure is possibly present on the entire surface of the sample. However, the domain structure in the remaining region could not be detected due to surface roughness. The pattern shows the so-called star-like domains and it is characteristic for uniaxial materials observed on the basal plane of single crystals Nd₂Fe₁₄B [10-11]. The observed type of domain structure indicates good magnetic texture for a permanent magnet. In few cases we found that magnetic domains were extended over the grain boundaries into neighboring grains, which could be attributed to the exchange interactions between the grains. Similar situation is observed for example in the article [12].

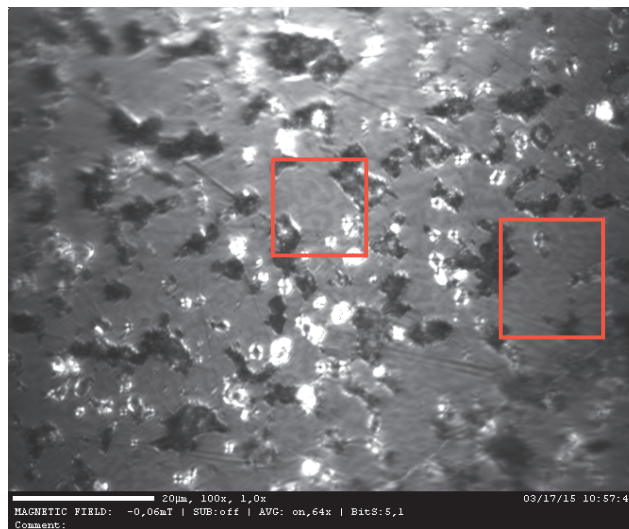


Fig. 4 The specimen surface of a permanent magnet N1 observed in a polarized light. Red squares highlight the areas with a magnetic domain structure. Magnetic field: -0.07 mT

4. CONCLUSIONS

The liquid phase sintering process was optimized by adding neodymium hydride. Optimal modes of heat treatment were determined. It was possible to increase the coercivity force of permanent magnets by forming continuous grain boundaries. As a result of the experiment, the samples of the high-coercivity magnet having the following magnetic properties: $H_{CJ} = >1470 \text{ kA}\cdot\text{m}^{-1}$, $B_r = 1.1 \text{ T}$ and $(BH)_{\text{max}} = 231 \text{ kJ}\cdot\text{m}^{-3}$ were obtained.

ACKNOWLEDGEMENTS

This paper was created in the project No. LO1203 „Regional Materials Science and Technology Centre - Feasibility Program” funded by Ministry of Education, Youth and Sports.

REFERENCES

- [1] LIU W.Q., SUN H., YI X.F., LIU X.C., ZHANG D.T., YUE M., ZHANG J.X. Coercivity enhancement in Nd-Fe-B sintered permanent magnet by Dy nanoparticles. Journal of Alloys and Compounds, Vol. 501, No. 1, 2010, pp. 67-69.

- [2] KOLCHUGINA N.B., LUKIN A., BURKHANOV G.S., SKOTNICOVÁ K., DRULIS H., PETROV V. Role of terbium hydride additions in the formation of microstructure and magnetic properties of sintered Nd-Pr-Dy-Fe-B magnets. In Metal 2012: 21th International Conference on Metallurgy and Materials. May 23rd-25th 2012 Brno, Czech Republic. 1st ed. Ostrava: Tanger s.r.o., 2012, pp. 1387-1392.
- [3] VIAL F., JOLY F., NEVALAINEN E., SAGAWA M., HIRAGA K., PARK K.T. Improvement of coercivity of sintered NdFeB permanent magnets by heat treatment. Journal of Magnetism and Magnetic Materials, Vol. 242-245, 2002, pp. 1329-1334.
- [4] KOSHKID'KO Yu.S., SKOTNICOVÁ K., KURSA M., ČEGAN T., BURKHANOV G.S., KOLCHUGINA N.B., LUKIN A.A., DORMIDONTOV A.G., SITNOV V.V. The effect of heat treatment under various conditions on microstructure of sintered (Nd,Pr,Dy)-Fe-B magnets. In METAL 2014: 23rd International Conference on Metallurgy and Materials, Conference Proceedings May 21nd-23rd 2014 Brno, Czech Republic. 1st ed. Ostrava: Tanger s.r.o., 2014, pp. 1369-1374.
- [5] BAI G., GAO R.W., SUN Y., HAN G.B., WANG B. Study of high-coercivity sintered NdFeB magnets. Journal of Magnetism and Magnetic Materials, Vol. 308, No. 1, 2007, pp. 20-23.
- [6] POHLUDKA M., MALCHARCZIKOVÁ J., MICHENKA V., KURSA M., ČEGAN T., SZURMAN I. Structure and mechanical properties of nickel alloys. In Metal 2013: 22th International Conference on Metallurgy and Materials. May 15th-17th 2012 Brno, Czech Republic. 1st ed. Ostrava: Tanger s.r.o., 2013, pp. 1567-1572.
- [7] KIM T.H., LEE S.R., NAMKUMG S., et al. A study on the Nd-rich phase evolution in the Nd-Fe-B sintered magnet and its mechanism during post-sintering annealing. Journal of Alloys and Compounds, Vol. 537, 2012, pp. 261-268.
- [8] WANG S.C., LI Y. In situ TEM study of Nd-rich phase in NdFeB magnet. Journal of Magnetism and Magnetic Materials, Vol. 285, No. 1-2, 2005, pp. 177-182.
- [9] WATANABE N., UMEMOTO H., ITAKURA M., NISHIDA M., MACHIDA K. Grain boundary structure of high coercivity Nd-Fe-B sintered magnets with Tb-metal vapor sorption. IOP Conf. Series: Materials Science and Engineering, Vol. 1, No. 1, 2009, p. 012033.
- [10] PASTUSHENKOV Yu.G., FORKL A., KRONMÜLLER H. Temperature dependence of the domain structure in Fe₁₄Nd₂B single crystals during the spin-reorientation transition. Journal of Magnetism and Magnetic Materials, Vol. 174, No. 3, 1997, pp. 278-288.
- [11] SUBKOVA A.V., ZEZIULINA P.A., KOSHKID'KO Yu.S., SIMONOV V.V., SKOKOV K.P., PASTUSHENKOV Yu.G. Temperature behaviour of magnetic domain structure in RE-3d intermetallics with spin-reorientation transitions. Solid State Phenomena, Vol. 168-169, 2011, pp. 122-125.
- [12] LÖEWE K., BROMBACHER C., KATTERB M., GUTFLEISCH O. Temperature-dependent Dy diffusion processes in Nd-Fe-B permanent magnets. Acta Materialia, Vol. 83, 2015, pp. 248-255.